High shear rheology of shear banding fluids in microchannels

Philippe Nghe,[1,a] Guillaume Degré,[1] Patrick Tabeling,[1] and Armand Ajdari[2]
[1]*Microfluidique, MEMs et Nanostructures, UMR Gulliver CNRS-ESPCI 7083, 10 rue Vauquelin, 75005 Paris, France*
[2]*Physico-Chimie Théorique, UMR Gulliver CNRS-ESPCI 7083, 10 rue Vauquelin, 75005 Paris, France*

(Received 3 October 2008; accepted 24 October 2008; published online 20 November 2008)

We characterize heterogeneous flows of a wormlike micelles solution in microchannels. Combining a pressure resistant microfabrication technology and a performant particle image velocimetry setup, we succeed in determining the nonlinear rheology of this fluid over 4 decades in shear rate and in particular more than 1 decade beyond the end of the stress plateau. We performed an independent measurement of the slip length with 1 μm resolution. © *2008 American Institute of Physics*. [DOI: 10.1063/1.3026740]

Semidilute solutions of wormlike micelles, which are used for enhanced oil recovery, cosmetics, and other detergent formulations, exhibit heterogeneous shear-banded flow,[1–3] spatiotemporal complex dynamics,[4,5] and slippage at the wall.[6] Determining the rheology of such fluids in a broad range of shear rates is, however, important from the practical point of view and still challenging. The reason is the presence of various instabilities triggered by the onset of shear banding or induced by the presence of curvature in classical rheometers.[7] Recent improvement in velocimetry techniques inside of rheometers[8–10] and investigations in rectilinear geometries[6,11] did not reach shear rates well beyond the end of the stress plateau. To achieve this goal, we extend the method described in Ref. 11 by using a performant microparticle image velocimetry setup combined with a pressure resistant microfabrication technology. Applying this to a cetyltrimethylammonium bromide (CTAB) solution, we are able to explore the second branch of the nonlinear rheology over more than 1 decade in terms of shear rates and under controlled flow conditions. The same experiment also provides information on the slippage at the wall. The technique we present here may also apply to complex fluids other than wormlike micelles, characterizing over a large dynamical range the nonlinear rheology.

The microsystem is a cross-rectangular channel of large aspect ratio (67 μm of height, 1 mm of width, and 4.5 cm of length) molded in a photocurable glue (NOA-81 Norland Products) on a glass slide, according to a microfabrication method described elsewhere.[12] As a result, the bottom surface is made of glass and the top and lateral walls are made of glue. This device can handle up to 6 bars of differential pressure without significant deformation (thickness variations of less than 1 μm). The inlet and the outlet are holes performed perpendicular to the extremities of the channel connected to pressurized reservoirs of centimeter scale. The channel can be moved in the x-y plane with an automated table (Marzhäuser) with a 1 μm resolution. The observation of the flow inside of the microchannel is realized through an inverted fluorescence microscope with a 100× oil immersion objective of large numerical aperture (NA=1.3), giving a focal depth of around 1 μm, mounted on a piezo to control its position in the height z with a 10 nm resolution. Illumination is made with a 300 mW laser of 532 nm wavelength, the beam going through an acousto-optic device used as a microsecond shutting system, and a 10× beam expander before entering into the optical microscope (Fig. 1). The data are acquired via a charged-coupled device camera (Allied), recorded with a direct-to-disk computer system (R&D Vision). In these conditions, the minimum time between two correlated images is 33 μs and the maximum measurable velocity in the microchannel is 0.1 m s^{-1}. At a given height z, 2000 images are captured (during several seconds), resulting in 1000 velocity measurements computed by intensity cross correlation between two images of 36×36 μm^2. The velocities and their error bars correspond, respectively, to the mean and the standard deviation of these measurements.

The fluid under study is a 0.3M CTAB solution in a 0.405M sodium nitrate ($NaNO_3$) brine. This solution is seeded with 500 nm fluorescent tracers (Duke) with a volume fraction below 10^{-4} to not perturb the flow behavior.

We perform velocity measurements across the height of the channel at different driving pressures (Fig. 2), ranging from 0.2 to 3.8 bars. The measurements shown in Fig. 2 are carried out in the middle of the width at 1 cm from the inlet of the channel. We observe a parabolic profile characteristic of Newtonian flow below 1.5 bars and shear bands become

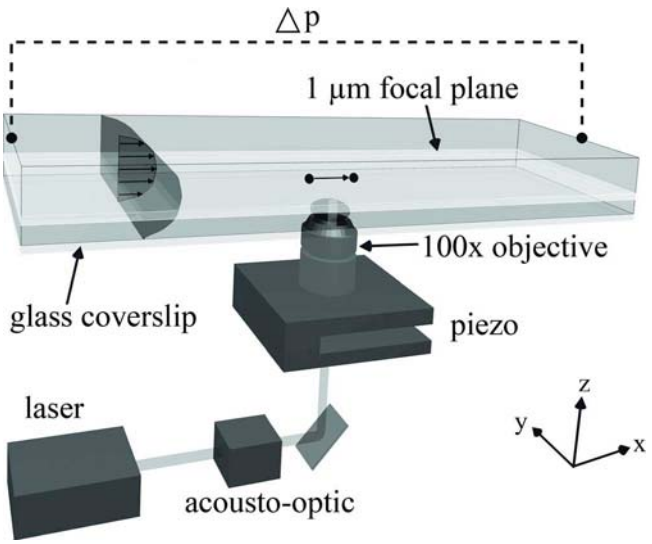

FIG. 1. (Color online) Sketch of the experimental setup.

[a]Electronic mail: philippe.nghe@espci.fr.

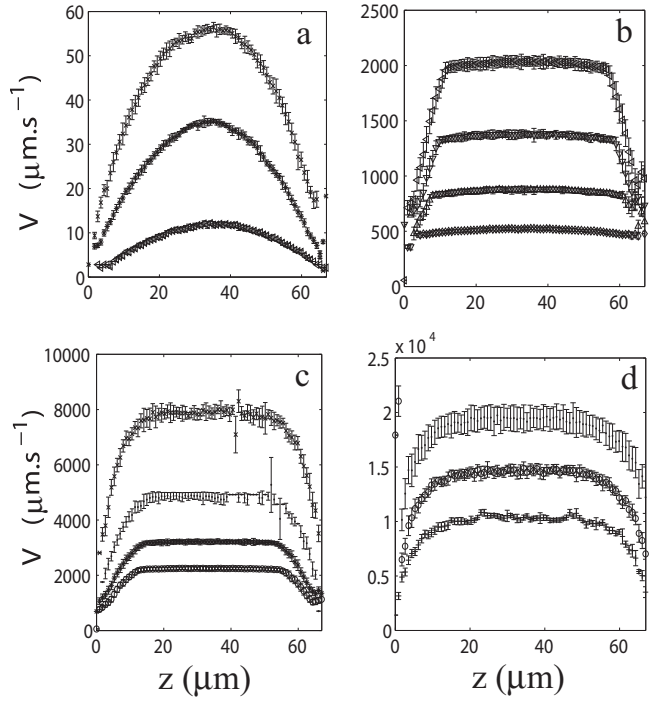

FIG. 2. Velocity profiles for a CTAB 0.3*M* in $NaNO_3$ 0.405*M* solution at a temperature of 26 °C measured in the middle of the width of the channel at 1 cm from the inlet in the flow direction. Increasing maximum velocities correspond to increasing pressures drops: (a) 0.4/1/1.4 bars, (b) 1.8/2/2.2/2.4 bars, (c) 2.5/2.7/2.9/3.1 bars, and (d) 3.2/3.4/3.8 bars.

visible close to the walls above this critical pressure. The stress at the wall at this pressure corresponds to the stress plateau value. The error bars are small and consistent with the absence of flow instability. We verify the invariances along x and y expected from the high aspect ratios and the absence of entry effects by performing series of velocity measurements at 1, 2, 3, and 3.8 bars in the middle of the width of the channel at different positions along the flow direction (1, 2, and 3 cm from the inlet), and in the first hundred microns around the channel symmetry axis in the direction of the side walls. The profiles obtained at these various locations collapse. Note however that approaching the channel end, the noise increases, perhaps a sign of spatiotemporal fluctuations that we wish to explore elsewhere. In any case the levels remain low and do not seem to affect the mean velocity profile.

In order to obtain the nonlinear rheology, we use, additionally to velocity measurements, the pressure differences Δp between the inlet and the outlet of the channel, neglecting the contribution of these two regions.[11,13] We extend the argument of Ref. 11 to a calculation in three dimensions, showing the result to be independent of the presence of lateral walls. At small Reynolds numbers, Stokes equation gives

$$\nabla p = \mathrm{div}(\sigma). \tag{1}$$

The experimentally observed invariance along the flow direction x of the velocity profile implies $\forall i,j,\ \partial_x \sigma_{ij}=0$. Applied to Stokes we get $\nabla(\partial_x p)=0$, in other words $\partial_x p$ is uniform through the whole channel of length L and equals $\Delta p/L$ by integration. The projection of the Stokes equation on the x axis is now

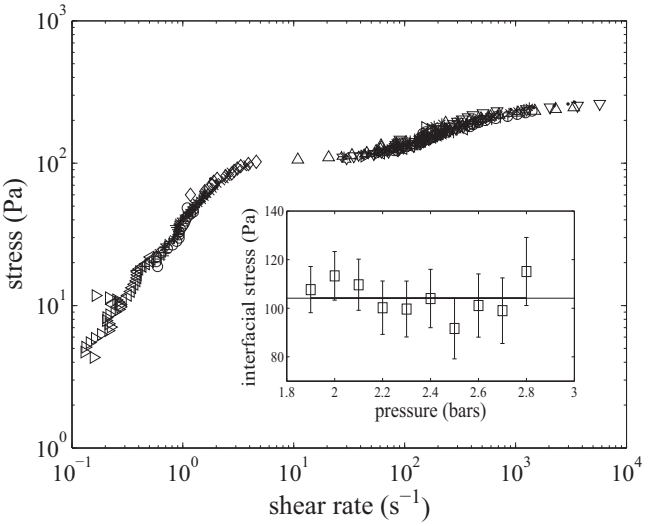

FIG. 3. Stress vs shear rate relation obtained from the velocity profiles of Fig. 2 with corresponding symbols and from velocity profiles at intermediary driving pressures (not represented on Fig. 2 for clarity). The insert represents the value of the stress at the interface between the shear bands extracted from the profiles of Figs. 2(b) and 2(c), the line representing the mean of these values.

$$\frac{\Delta p}{L} = \partial_y \sigma_{xy} + \partial_z \sigma_{xz}. \tag{2}$$

At this point, regardless of the aspect ratio of the channel and for symmetry reasons, the integration of Eq. (2) in the middle of the width results in

$$\sigma_{xz} = \frac{\Delta p}{L}(z - z_0) \tag{3}$$

with z_0 as the height at which the shear rate equal zero. In our case, the velocity profiles change very slowly along the width y in a large zone around the middle of the channel, therefore $\partial_y \sigma_{xy} \ll \partial_z \sigma_{xz}$ and Eq. (3) remains true in this zone by integration of Eq. (2). At a given driving pressure, we obtain a local shear rate by derivation of the velocity profile and finally map $\sigma(z)$ versus $\dot{\gamma}(z)$ for each z. Applying this method to the velocity profiles of Fig. 2, we succeed in collapsing the curves obtained for each driving pressure on a master curve that represents the nonlinear rheology of the CTAB solution (Fig. 3) for shear rates ranging from 0.1 to several 1000 s^{-1} under controlled conditions; let us underline that the rheology is obtained independently from the slippage at the wall, this estimate being purely local to each z value. The collapse of the different curves indicates that a local rheology accounts for describing the flow of this solution in our experiment. The master curve obtained has two branches separated by a stress plateau as expected for such shear-banding solution. The second branch is obtained over more than a decade of shear rates and indicates a strongly shear-thinning behavior.

We then characterize the wall slip by extrapolating the velocity profiles obtained over a few microns above the glass wall to the z value giving a zero velocity. The wall position is obtained separately by measuring the position of a tracer adsorbed on the glass surface with a submicrometric resolution.[14] We plot the measured slip length versus the wall shear rates obtained for driving pressures ranging from 1.8 to 3.2 bars (Fig. 4), which correspond to the shear-banding re-

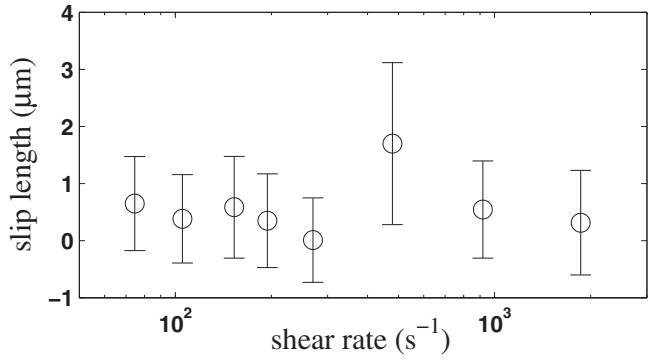

FIG. 4. Slip length vs shear rate at the wall in the shear-banding regime, for driving pressures ranging from 1.8 to 3.2 bars.

gime. These measurements indicate no significant slippage above our error and no evolution with the shear rate at the wall. The mean of all these data is 0.5 ± 0.9 μm of slip length.

We have been able to characterize the nonlinear rheology of a semidilute solution of wormlike micelles, measuring the stress over more than one order of magnitude of deformation rates for the branch above the stress plateau, estimating at the same time the slip length to be below the micron scale. More generally, this work shows how we can get under controlled conditions the nonlinear rheology for viscous fluids prone to unstable behavior in classical rheometers using (as in any microfluidic system) extremely small amounts of fluids.

To conclude, we make the following comments on some physical implications of these measurements. The shape of the second branch of the rheology on Fig. 3 shows that a simple power law is not sufficient to describe the behavior of the high shear phase of the CTAB solution. There is a need for theoretical models that could account for this yet uninterpreted behavior.[15] Interestingly, if we omit the curvature of the rheological curve and use a power law fit restricted to the proximity of the plateau region (from 100 to 300 s^{-1}), one obtains an exponent of 0.26 for a scaling law of stress versus shear rate, which is compatible with recent Couette rheometer measurements on the same fluid.[16]

At different pressures in the shear-banding regime, we measure directly on the velocity profiles the position of the interface between the two bands and deduce from relation (3) the corresponding stress (insert in Fig. 3). In a range of deformation rates up to 300 s^{-1}, this stress is located at a constant level consistently with the value of the stress plateau of the collapsed rheological curves. This provides no sign for the importance of nonlocal terms that could play a role in the rheology of our fluid. Nonlocal effects have been seen in experiments on the same fluids[6] in different microchannels. The compatibility of these observations needs further analysis.

A more detailed study of the velocity profiles along the width shows that secondary patterns with a wavevector in the y axis direction develop downstream, consistent with theoretical predictions[17] and observations made in a Couette geometry.[4] In our case, these instabilities have a very small amplitude and do not seem to affect the time averaged quantities we measure, from which rheology is inferred. We are now exploring the complex spatiotemporal behavior exhibited by such fluids in our particular rectilinear geometry.

The authors acknowledge Total Petrochemicals for funding this research.

[1]M. M. Britton and P. T. Callaghan, Phys. Rev. Lett. **78**, 4930 (1997).
[2]J. F. Berret, G. Porte, and J. P. Decruppe, Phys. Rev. E **55**, 1668 (1997).
[3]S. Lerouge, J. P. Decruppe, and C. Humbert, Phys. Rev. Lett. **81**, 5457 (1998).
[4]S. Lerouge, M. Argentina, and J. P. Decruppe, Phys. Rev. Lett. **96**, 088301 (2006).
[5]L. Becu, D. Anache, S. Manneville, and A. Colin, Phys. Rev. Lett. **93**, 018301 (2004).
[6]C. Masselon, J. B. Salmon, and A. Colin, Phys. Rev. Lett. **100**, 038301 (2008).
[7]J. F. Berret, D. C. Roux, and G. Porte, J. Phys. II **4**, 1261 (1994).
[8]M. M. Britton and P. T. Callaghan, Eur. Phys. J. B **7**, 237 (1999).
[9]S. Manneville, L. Becu, and A. Colin, Eur. Phys. J. Appl. Phys. **28**, 361 (2004).
[10]J. B. Salmon, A. Colin, S. Manneville, and F. Molino, Phys. Rev. Lett. **90**, 228303 (2003).
[11]G. Degre, P. Joseph, P. Tabeling, S. Lerouge, M. Cloitre, and A. Ajdari, Appl. Phys. Lett. **89**, 024104 (2006).
[12]D. Bartolo, G. Degre, P. Nghe, and V. Studer, Lab Chip **8**, 274 (2008).
[13]H. Mullermohnssen, D. Weiss, and A. Tippe, J. Rheol. **34**, 223 (1990).
[14]P. Joseph and P. Tabeling, Phys. Rev. E **71**, 035303 (2005).
[15]P. D. Olmsted, Rheol. Acta **47**, 283 (2008).
[16]S. Lerouge, M. A. Fardin, M. Argentina, G. Grégoire, and O. Cardoso, Soft Matter **4**, 1808 (2008).
[17]S. M. Fielding, Phys. Rev. E **76**, 016311 (2007).